Synthesis and Structure of Titanatranes Containing Tetradentate Trianionic Donor Ligands of the Type $[(O\text{-}2,4\text{-}R_2C_6H_2\text{-}6\text{-}CH_2)_2(OCH_2CH_2)]N^{3-}$ and Their Use in Catalysis for Ethylene Polymerization

Sudhakar Padmanabhan, Shouhei Katao, and Kotohiro Nomura*

Graduate School of Materials Science, Nara Institute of Science and Technology (NAIST), 8916-5 Takayama, Ikoma, Nara 630-0101, Japan

Received December 19, 2006

Syntheses and structural characterizations of various titanatranes containing bis(aryloxo)ethanolamine ligands of the type $[(O\text{-}2,4\text{-}R_2C_6H_2\text{-}6\text{-}CH_2)_2(OCH_2CH_2)]N^{3-}$ (R = Me, ^{t}Bu) have been explored. The reaction of $[(HO\text{-}2,4\text{-}Me_2C_6H_2\text{-}6\text{-}CH_2)_2(HOCH_2CH_2)]N$ with $Ti(OR')_4$ in toluene afforded dimeric titanatranes, $Ti_2(OR')_2\{[(O\text{-}2,4\text{-}Me_2C_6H_2\text{-}6\text{-}CH_2)_2(\mu_2\text{-}OCH_2CH_2)]N\}_2$ [R′ = ^{i}Pr (**1a**), ^{t}Bu (**1b**)], in high yields. Crystallographic analyses of **1a**,**b** indicate that these complexes have a distorted octahedral geometry around Ti, and the O atom in the alkoxo ligand is coordinated to two Ti atoms. The similar reactions of $[(HO\text{-}2,4\text{-}^tBu_2C_6H_2\text{-}6\text{-}CH_2)_2(HOCH_2CH_2)]N$ with $Ti(OR')_4$ afforded the monomeric titanatranes $Ti(OR')[(O\text{-}2,4\text{-}^tBu_2C_6H_2\text{-}6\text{-}CH_2)_2(OCH_2CH_2)]N$ (**2a**,**b**) in high yields; these complexes have a rather distorted trigonal bipyramidal structure around Ti consisting of a plane formed by two aryloxo and one alkoxo ligand and an N−Ti−O (in O^{t}Bu) axis determined by the X-ray crystallographic analyses. The reaction of **1a**,**b** with 2.0 equiv of $AlMe_3$ (1.0 equiv per Ti) in toluene gave the Ti−Me complexes coordinated to $Me_2Al(OR')$, $\{TiMe[(O\text{-}2,4\text{-}Me_2C_6H_2\text{-}6\text{-}CH_2)_2(\mu_2\text{-}OCH_2CH_2)N]\}[Me_2Al(\mu_2\text{-}OR')]$ [R′ = ^{i}Pr (**3a**), ^{t}Bu (**3b**)], in exclusive yields, and these complexes were identified by ^{1}H and ^{13}C NMR spectra, elemental analyses, and X-ray crystallography. Complexes **1a** and **2b** exhibited moderate catalytic activities for ethylene polymerization at 100−120 °C in the presence of methylaluminoxane (MAO), and the activity increased upon the addition of a small amount of $AlMe_3$. Similar catalytic activities were observed by using **3a**,**b** in the presence of MAO, affording high molecular weight polyethylene with unimodal molecular weight distributions. Ethylene polymerization in octane by **3b** took place without additional cocatalyst at 120 °C with moderate catalytic activity (94 kg PE/mol Ti·h), affording high molecular weight polymer with unimodal distribution ($M_w = 1.00 \times 10^6$, $M_w/M_n = 2.58$). The result clearly suggests that the cationic species formed by cleavage of the Ti−O bonds plays an important role as the active species for the polymerization.

Introduction

Considerable attention has been paid to the chemistry of metal complexes containing tripodal trianionic ligands such as triamido, tris(amido)amine, tris(alkoxo)amine, and tris(aryloxo)-amine.[1−18] Especially complexes with triamido or tris(amido)-amine ligands displayed unique characteristics.[2] These trianionic, chelating amido and/or alkoxo ligands are capable of providing a range of stable steric and electronic environments for catalytically active metal centers and have thus been the subject of considerable attention.[2] Schrock recently demonstrated the

* Corresponding author. Tel: +81-743-72-6041. Fax: +81-743-72-6049. E-mail: nomurak@ms.naist.jp.

(1) Cohen, H. J. *J. Organomet. Chem.* **1966**, *5*, 413−419.

(2) (a) Verkade, J. G. *Acc. Chem. Res.* **1993**, *26*, 483−489. (b) Schrock, R. R. *Acc. Chem. Res.* **1997**, *30*, 9−16. (c) Cummins, C. C. *Chem. Commun.* **1998**, 1777−1786. (d) Gade, L. H. *Chem. Commun.* **2000**, 173−181. (e) Gade, L. H. *Acc. Chem. Res.* **2002**, *35*, 575−582. (f) Gibson, S. E.; Castaldi, M. P. *Chem. Commun.* **2006**, 3045−3062.

(3) (a) Nugent, W. A. *J. Am. Chem. Soc.* **1992**, *114*, 2768−2769. (b) Nugent, W. A.; Harlow, R. L. *J. Am. Chem. Soc.* **1994**, *116*, 6142−6148. (c) Furia, F. D.; Licini, G.; Modena, G.; Motterle, R.; Nugent, W. A. *J. Org. Chem.* **1996**, *61*, 5175−5177. (d) Bonchio, M.; Calloni, S.; Furia, F. D.; Licini, G.; Modena, G.; Moro, S.; Nugent, W. A. *J. Am. Chem. Soc.* **1997**, *119*, 6935−6936. (e) Nugent, W. A. *J. Am. Chem. Soc.* **1998**, *120*, 7139−7140. (f) Bonchio, M.; Licini, G.; Modena, G.; Bortolini, O.; Moro, S.; Nugent, W. A. *J. Am. Chem. Soc.* **1999**, *121*, 6258−6268.

(4) Lütjens, H.; Wahl, G.; Möller, F.; Knochel, P.; Sundermeyer, J. *Organometallics* **1997**, *16*, 5869−5878.

(5) Moberg, C. *Angew. Chem., Int. Ed.* **1998**, *37*, 248−268.

(6) (a) Kim, Y.; Hong, E.; Lee, M. H.; Kim, J.; Han, Y.; Do, Y. *Organometallics* **1999**, *18*, 36−39. (b) Kim, Y.; Han, Y.; Hwang, J.-W.; Kim, M. W.; Do, Y. *Organometallics* **2002**, *21*, 1127−1135. (c) Lee, K.-S.; Kim, Y.; Ihm, S.-K.; Do, Y.; Lee, S. *J. Organomet. Chem.* **2006**, *691*, 1121−1125. (d) Kim, Y.; Do, Y. *J. Organomet. Chem.* **2002**, *655*, 186−191.

(7) Chandraekaran, A.; Day, R. O.; Holmes, R. R. *J. Am. Chem. Soc.* **2000**, *122*, 1066−1072.

(8) Jia, L.; Ding, E.; Rheingold, A. L.; Rhatigan, B. *Organometallics* **2000**, *19*, 963−965. The catalytic activity at 90 °C was extremely low (0.030 kg PE/mol Zr·h). The activity decreased at lower temperature.

(9) Kol, M.; Shamis, M.; Goldberg, I.; Goldschmidt, Z.; Alfi, S.; Hayut-Salant, S. *Inorg. Chem. Commun.* **2001**, *4*, 177−179.

(10) Bull, S. D.; Davidson, M. W.; Johnson, A. L.; Robinson, D. E. J. E.; Mahon, M. F. *Chem. Commun.* **2003**, 1750−1751.

(11) Michalczyk, L.; de Gala, S.; Bruno, J. W. *Organometallics* **2001**, *20*, 5547−5556.

(12) (a) Kim, Y.; Verkade, J. G. *Macromol. Rapid Commun.* **2002**, *23*, 917−921. (b) Kim, Y.; Jnaneshwara, G. K.; Verkade, J. G. *Inorg. Chem.* **2003**, *42*, 1437−1447. (c) Kim, Y.; Verkade, J. G. *Macromol. Symp.* **2005**, *224*, 105−117. (d) Kim, Y.; Verkade, J. G. *Organometallics* **2002**, *21*, 2395−2399. (e) Kim, Y.; Verkade, J. G. *Inorg. Chem.* **2003**, *42*, 4804−4806. (f) Su, W.; Kim, Y.; Ellern, A.; Guzei, I. A.; Verkade, J. G. *J. Am. Chem. Soc.* **2006**, *128*, 13728−13735.

(13) Verkerk, U.; Fujita, M.; Dzwiniel, T. L.; McDonald, R.; Stryker, J. M. *J. Am. Chem. Soc.* **2002**, *124*, 9988−9989.

(14) Matsuo, T.; Kawaguchi, H. *Inorg. Chem.* **2002**, *41*, 6090−6098.

(15) Maestri, A. G.; Brown, S. N. *Inorg. Chem.* **2004**, *43*, 6995−7004.

10.1021/om0611507 CCC: $37.00
Publication on Web 02/22/2007

Chart 1

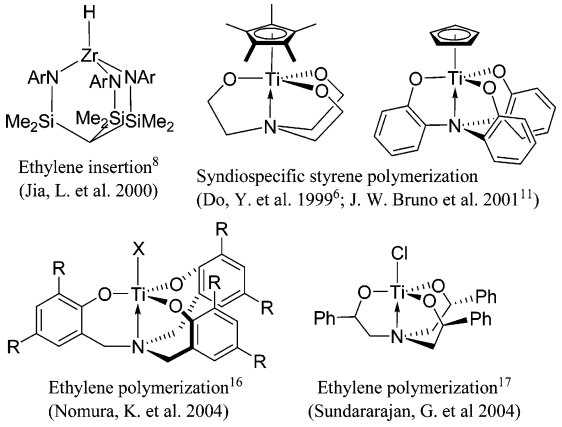

catalytic dinitrogen activation using molybdenum complexes,[18] and Kol reported that titanium complexes containing tris(aryloxo)amine ligands, which form well-defined mononuclear trigonal bipyramidal structures with C_3 symmetry, exhibited high barriers to inversion and differences in shielding of the axial ligand.[9] Gibson et al. reviewed various C_3 symmetric titanatranes, which are very effective for organometallic reactions.[2f]

Examples applied to catalysis for organic synthesis[2f,3,10] as well as for polymerization[6a,b,11,12b−d,16,17] have been known,[2f] and the zirconium benzyl and hydride complexes with triamido ligand incorporated ethylene at 70−90 °C (Chart 1).[8] Reports for syndiospecific styrene polymerization by Cp*Ti[$(OCH_2CH_2)_3$N]−[6a,b] and CpTi[$(O\text{-}2\text{-}C_6H_4)_3$N][11]−methylaluminoxane (MAO) catalysts are also known;[19] however, no examples concerning efficient catalysts for olefin polymerization had been reported until recently.[16,17] In addition, the catalytic activities for lactide polymerization initiated by titanatrans were low even at 130 °C.[12b−d] Since the design and synthesis of efficient transition metal complex catalysts toward controlled olefin polymerization attract considerable attention in the field of organometallic chemistry, catalysis, and polymer chemistry,[20] we thus had an interest in exploring the possibility of using titanatrans as the new candidates. We especially focused on use of aryloxide moieties partially as the ligands, because we reported that half-titanocenes[21] and (arylimido)vanadium complexes[22] containing aryloxide ligands displayed unique characteristics as olefin polymerization catalysts.

We recently communicated that some titanium aryloxide/isopropoxide complexes containing a tris(aryloxo)amine ligand, TiX[$(O\text{-}2,4\text{-}R_2C_6H_2\text{-}6\text{-}CH_2)_3$N] [R = Me, ^{t}Bu; X = O^{i}Pr, O-2,6-$^i Pr_2C_6H_3$], were effective as catalyst precursors for ethylene polymerization in the presence of MAO, and the activities remarkably increased at higher temperature even at 100−120 °C.[16] The activity also increased upon addition of a small amount of $AlMe_3$.[16] Since $AlMe_3$ itself did not initiate the ethylene polymerization, the role for improving the efficiency of generating catalytically active species (alkyl cationic species containing a chelate bidentate donor ligand), presumably formed by dissociation of one of three Ti−O bonds by $AlMe_3$, might be thus assumed.[23] The related examples, (chloro)titanium complexes containing C_3 and C_s symmetric tris(alkoxo)amine ligands of the type $[OCH(Ph)CH_2]_3N^{3-}$, were also introduced later,[17] and the 1-hexene polymerization by a C_3 symmetric complex proceeded in an isospecific manner in the presence of MAO. On the basis of the previous results,[16] we thus focused on titanatranes containing bis(aryloxo)-(alkoxo)amine ligands of the type [$(O\text{-}2,4\text{-}R_2C_6H_2\text{-}6\text{-}CH_2)_2(OCH_2CH_2)]N^{3-}$ (R = Me, ^{t}-Bu), as promising candidates for catalyst precursors for olefin polymerization. We expected that the rigid framework provided by the aryloxo arms is more stable than the alkoxo arm, and the alkoxo arm would thus be cleaved by addition of Al cocatalyst to afford the cationic species, which are expected to be catalytically active for ethylene polymerization. In this paper, we thus wish to present syntheses and structural characterizations of titanatranes containing trianionic donor ligands and their use in catalysis for ethylene polymerization. Since the observed catalytic activity increased upon addition of $AlMe_3$, we have explored the role of $AlMe_3$ including isolation and characterization of the intermediate.[24]

Results and Discussion

1. Synthesis, Identification, and Structural Determination of Various Titanatranes Containing [$(O\text{-}2,4\text{-}R_2C_6H_2\text{-}6\text{-}CH_2)_2(OCH_2CH_2)]N^{3-}$ (R = Me, ^{t}Bu) Ligands. The general scheme for the synthesis of titanatranes containing bis(aryloxo)-(alkoxo)-amine ligands of the type [$(O\text{-}2,4\text{-}R_2C_6H_2\text{-}6\text{-}CH_2)_2(OCH_2CH_2)]N^{3-}$ [R = Me (**1**), ^{t}Bu (**2**)] is shown in Scheme 1. The reaction of [$(HO\text{-}2,4\text{-}Me_2C_6H_2\text{-}6\text{-}CH_2)_2(HOCH_2CH_2)$N] (**Lig 1**) with Ti(O^{i}Pr)$_4$ in toluene gave a dimeric titanatrane, $Ti_2(O^iPr)_2${[(O-

(16) Wang, W.; Fujiki, M.; Nomura, K. *Macromol. Rapid Commun.* **2004**, *25*, 504−507.

(17) (a) Sudhakar, P.; Amburose, C. V.; Sundararajan, G.; Nethaji, M. *Organometallics* **2004**, *23*, 4462−4467. (b) Sudhakar, P.; Sundararajan, G. *Macromol. Rapid Commun.* **2005**, *26*, 1854−1859.

(18) (a) Yandulov, D. V.; Schrock, R. R. *Science* **2003**, *301*, 76−78. (b) Schrock, R. R. *Acc. Chem. Res.* **2005**, *38*, 955−962. The catalytic reduction of dinitrogen by molybdenum complexes that contain the $[HIPTN_3N]^{3-}$ ligand ($[HIPTN_3N]^{3-}$ = $[(HIPTNCH_2CH_2)_3N]^{3-}$, where HIPT = 3,5-(2,4,6-$^i Pr_3C_6H_2)_2C_6H_3$) at room temperature and pressure with protons and electrons.

(19) Although the mechanistic implications in this catalysis for styrene polymerization should be important, no detailed mechanistic insights were described.[6,11] This is because it has been proposed that the cationic Ti(III)-containing cyclopentadienyl group is generated by dissociation of the $[(OCH_2CH_2)_3N]^{3-}$ ligand and plays an important role as the catalytically active species. Examples of a mechanistic study for styrene polymerization (and propylene/styrene copolymerization): (a) Grassi, A.; Zambelli, A.; Laschi, F. *Organometallics* **1996**, *15*, 480−482. (b) Mahanthappa, M. K.; Waymouth, R. M. *J. Am. Chem. Soc.* **2001**, *123*, 12093−12904. (c) Minieri, G.; Corradini, P.; Guerra, G.; Zambelli, A.; Cavallo, L. *Macromolecules* **2001**, *34*, 5379−5385.

(20) (a) *Ziegler Catalysts*; Fink, G., Mulhaupt, R., Brintzinger, H. H., Eds.; Springer: Berlin, 1995. For review articles on metallocene and non-metallocene based catalysts for olefin polymerization: (b) Brintzinger, H. H.; Fischer, D.; Mülhaupt, R.; Rieger, B.; Waymouth, R. M. *Angew. Chem., Int. Ed. Engl.* **1995**, *34*, 1143−1170. (c) McKnight, A. L.; Waymouth, R. M. *Chem. Rev.* **1998**, *98*, 2587. (d) Alt, H. G.; Köppl, A. *Chem. Rev.* **2000**, *100*, 1205−1222. (e) Resconi, L.; Cavallo, L.; Fait, A.; Piemontesi, F. *Chem. Rev.* **2000**, *100*, 1253−1346. (f) Chen, E. Y-X.; Marks, T. J. *Chem. Rev.* **2000**, *100*, 1391−1434. (g) Gibson, V. C.; Spitzmesser, S. K. *Chem. Rev.* **2003**, *103*, 283−316.

(21) For example: (a) Nomura, K.; Liu, J.; Padmanabhan, S.; Kitiyanan, B. *J. Mol. Catal. A*, in press (Review). (b) Nomura, K.; Naga, N.; Miki, M.; Yanagi, K.; Imai, A. *Organometallics* **1998**, *17*, 2152−2154. (c) Nomura, K.; Komatsu, T.; Imanishi, Y. *Macromolecules* **2000**, *33*, 8122−8124.

(22) For example: (a) Nomura, K.; Sagara, A.; Imanishi, Y. *Macromolecules* **2002**, *35*, 1583−1590. (b) Wang, W.; Nomura, K. *Macomolecules* **2005**, *38*, 5905−5913. (c) Wang, W.; Nomura, K. *Adv. Synth. Catal.* **2006**, *348*, 743−750.

(23) The above complexes, TiX[$(O\text{-}2,4\text{-}R_2C_6H_2\text{-}6\text{-}CH_2)_3$N] [R = Me, ^{t}Bu; X = O^{i}Pr, O-2,6-$^i Pr_2C_6H_3$], did not show any catalytic activities for syndiospecific styrene polymerization,[16] although some half-titanocenes containing tris(alkoxo)amine ligands showed moderate catalytic activities.[6a,b] The results suggested that the role of the cyclopentadienyl fragment rather than the tris(alkoxo)amine or tris(aryloxo)amine ligand is dominant for syndiospecific styrene polymerization.

(24) Reaction of Ti−alkoxides containing a tridentate (OSO) [OSO = 2,2′-thiobis{4-(1,1,3,3-tetramethylbutyl)phenoxy} ligand with $AlMe_3$: Janas, Z.; Jerzykiewicz, L. B.; Sobota, P.; Szczegot, K.; Wiceniewska, D. *Organometallics* **2005**, *24*, 3987−3994.

Scheme 1

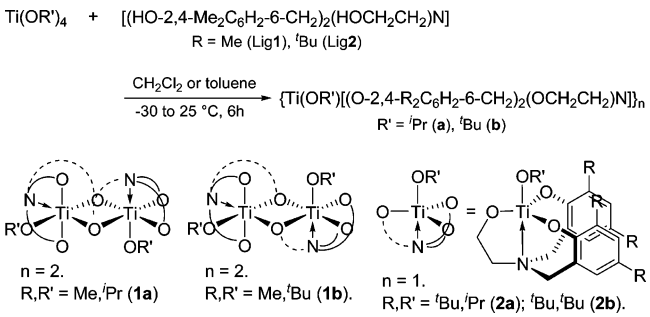

2,4-$R_2C_6H_2$-6-$CH_2)_2(\mu_2$-$OCH_2CH_2)N]\}_2$ (**1a**), in high yield (86.0%). Complex **1a** could be identified by ^{1}H and ^{13}C NMR spectra and elemental analysis, and the structure was determined by X-ray crystallography.

The crystallographic analysis of **1a** shown in Figure 1 (left) indicates that **1a** has a distorted octahedral geometry around each Ti center and possesses a dimeric structure. The oxygen on the ethoxy arm is bound to the two titanium atoms, stabilizing these systems in the dimeric form. The bond lengths between titanium and oxygen indicate that the Ti−O bond distances bound to the two titanium centers are influenced by the ligand in the *trans* position [N(1) vs O(6); Ti(1)−O(7), Ti(2)−O(7) = 1.986, 2.081 Å, respectively], as shown in Table 1. These bond distances are, however, somewhat longer than those in alkoxides [1.812(2), 1.778(3) Å], as well as in aryloxides [1.855(2)−1.922(2) Å], although these distances (Ti−O in alkoxides, aryloxides) are also influenced by the ligands coordinated in the *trans* position. Ti−O bond distances in the aryloxides are somewhat longer than those in Cp′TiX_2(OAr) reported previously (Ti−O = 1.772−1.811 Å),[21a,b] probably due to the stabilization of the dimeric structure. The isopropoxide ligand is bound to one titanium center, and the distances are also influenced by the ligand in the *trans* position [O(3) vs N(2), Ti(1)−O(4), Ti(2)−O(8) = 1.812(2), 1.778(3), respectively]. Ti−N bond distances are also influenced by the ligand coordinated in the *trans* position [Ti(1)−N(1) (*trans* to bridged oxygen), Ti(2)−N(2) (*trans* to O^{i}Pr) = 2.258(3), 2.341(3) Å, respectively].

The ^{1}H NMR spectra of **1a** showed broad resonances at 25 °C, and the degree of each resonance was dependent upon the temperature measured, as shown in Figure 2a−c, and was influenced by the NMR solvent employed. VT NMR spectra (in $CDCl_3$, Figure 2a−d) of **1a** showed a sharpening of each signal measured at 60 °C. Probable assumptions for explaining the observations would be that the cleavage of poly- or oligonuclear into monomeric species occurred at elevated temperature or an equilibrium between dimeric and monomeric species. Another probable explanation would be the fluxional nature of methylene units in these ligands, because the ^{1}H NMR spectrum of **1a** in THF-d_8 at 25 °C did not show any improvement in sharpening the resonances. The latter explanation may be considered from the results in the ^{1}H NMR spectra for the monomeric titanatranes as described below, because similar temperature dependences were seen even in the spectra for the monomeric species.

In an attempt to isolate monomeric titanatrane, we reacted [(HO-2,4-$Me_2C_6H_2$-6-$CH_2)_2$($HOCH_2CH_2$)N] (**Lig 1**) with Ti(O^{t}Bu)$_4$ in toluene. This is an approach analogous to that reported by Verkade et al.[25] to prepare the monomeric titanatrane containing 2,6-diisopropylphenoxide; however, the dimeric titanatrane, Ti_2(O^{t}Bu)$_2$\{[(O-2,4-$R_2C_6H_2$-6-$CH_2)_2(\mu_2$-OCH_2-CH_2)N]\}$_2$ (**1b**), was isolated in high yield (81.8%). **1b** could be identified by ^{1}H and ^{13}C NMR spectra and elemental analysis, and the structure was determined by X-ray crystallography.

The crystallographic analysis of **1b** shown in Figure 1 (right) indicates that the structure of **1b** is somewhat analogous to that of **1a**; **1b** has a distorted octahedral geometry around each Ti center and the oxygen on the ethoxy arm is bound to the two titanium atoms, stabilizing these systems in the dimeric form. Apparent differences between **1a** and **1b** are the positions of nitrogen and oxygen in the OR′ ligands as depicted in Scheme 1 [N(2) and O(8) shown on the right], although no significant differences were observed in the bond distances and the angles between **1a** and **1b**. The observed differences in the dimeric structures would be explained by an assumption that the most stabilized forms may be different due to the influence of the rather bulky O^{t}Bu lignd in **1b**. The O^{t}Bu ligand is bound to one titanium metal center, and the distances are influenced by the ligand in the *trans* position [O(3) vs N(2), Ti(1)−O(4), Ti(2)−O(8) = 1.776(2), 1.751(3) Å, respectively]; the distances are somewhat shorter than those in **1a** (Ti−O^{i}Pr). As seen in the ^{1}H NMR spectra for **1a**, the ^{1}H NMR spectra of **1b** (Figure 2d−g) showed broad resonances at 25 °C (Figure 2g), and each resonance became sharp at 60 °C. These are analogous to those observed in **1a** (shown in Figure 2a−c).

In our continued effort to isolate monomeric titanatranes, we chose the reaction of Ti(OR′)$_4$ [R′ = ^{i}Pr (**a**), ^{t}Bu (**b**)] with [(HO-2,4-^{t}Bu$_2C_6H_2$-6-$CH_2)_2$($HOCH_2CH_2$)N] (**Lig 2**), because the increase of steric bulk around the phenoxy moiety, by replacement of the methyl with a *tert*-butyl group in the *ortho* position, might be effective to avoid the dimerization/oligomerization of monomeric titanium species.

The isolated product from the chilled toluene solution containing a reaction mixture of **Lig 2** and Ti(O^{i}Pr)$_4$ was **2a** in high yield (83.0%, Scheme 1). **2a** could be identified by ^{1}H and ^{13}C NMR spectra and elemental analysis, and the structure was determined as the monomeric form by X-ray crystallography (Figure 3, left). The similar reaction of **Lig 2** with Ti(O^{t}Bu)$_4$ also afforded **2b**, identified by ^{1}H and ^{13}C NMR spectra and elemental analysis, and the structure was determined as the monomeric form by X-ray crystallography.

The X-ray crystallographic analysis of **2a** (Figure 3, left) reveals that **2a** has a rather distorted trigonal bipyramidal structure around Ti; N and O in O^{i}Pr are located in a *trans* position to a plane consisting of two aryloxo and one alkoxo ligand, as evident from the O−Ti−N bond angle [O(1)−Ti(1)−N(1) 174.14(19)°] as well as the sum of bond angles around Ti [ca. 360°; O(2)−Ti(1)−O(3), 118.80(17)°; O(2)−Ti(1)−O(4), 117.12(17)°; O(3)−Ti(1)−O(4), 117.04(17)°], as shown in Table 2. The basic structure is somewhat similar to that in the titanatranes containing tris(aryloxo)amine ligands reported by Kol et al.[9] Bond distances in Ti−O (alkoxo) in **2a** are apparently shorter than those in **1a** [Ti(1)−O(2) 1.825(4) Å in **2a** vs Ti(1)−O(3), Ti(2)−O(7) 2.056(2), 2.081(2) Å in **1a**], and the bond distance for Ti−O^{i}Pr in **2a** is somewhat shorter than those in **1a** [1.770(3) Å in **2a** vs 1.812(2), 1.778(3) Å in **1a**]. These suggest that these alkoxide ligands strongly coordinate to the titanium. In contrast, the Ti−N bond distance in **2a** is longer than that in **1a** probably due to the strong *trans* influence in Ti−O^{i}Pr [Ti(1)−N(1) 2.328(3) Å in **2a** vs Ti(1)−N(1), Ti(2)−N(2) 2.258(3), 2.341(3) Å, respectively in **1a**].

The crystallographic analysis of **2b** (Figure 3, right) reveals that the basic structure in **2b** is analogous to **2a**. **2b** has a rather

(25) Menge, W. M. P. B.; Verkade, J. G. *Inorg. Chem.* **1991**, *30*, 4628−4631.

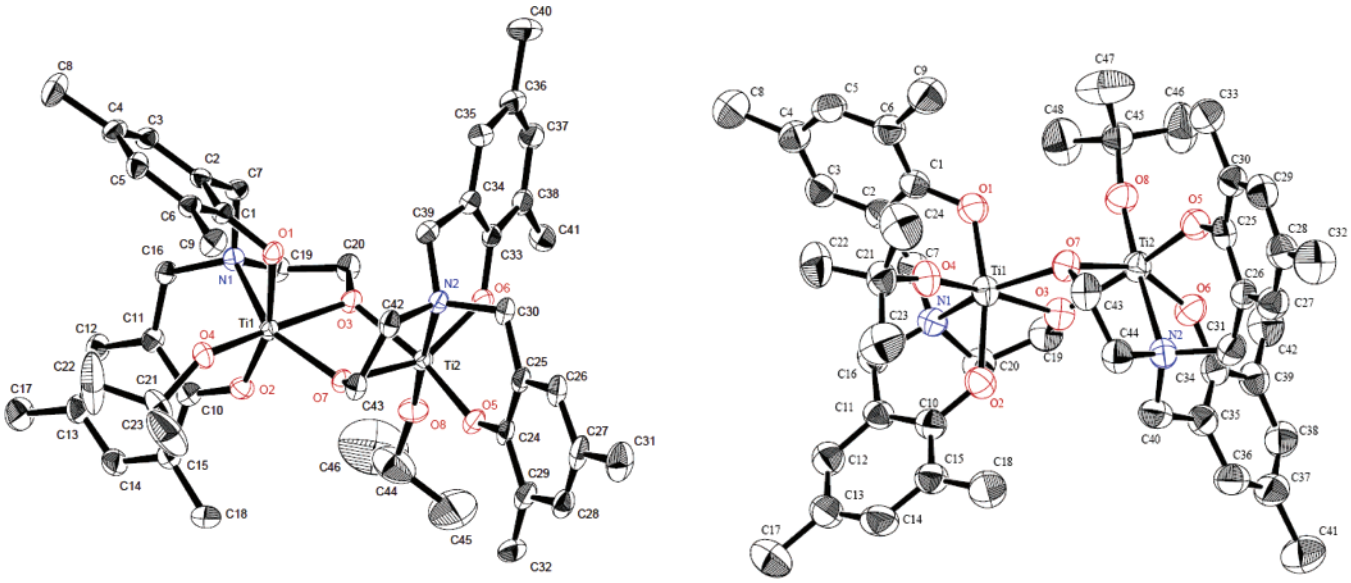

Figure 1. ORTEP drawings for $Ti_2(O^iPr)_2\{[(O\text{-}2,4\text{-}Me_2C_6H_2\text{-}6\text{-}CH_2)_2(\mu_2\text{-}OCH_2CH_2)N]\}_2$ (**1a**, left) and $Ti_2(O^tBu)_2\{[(O\text{-}2,4\text{-}Me_2C_6H_2\text{-}6\text{-}CH_2)_2(\mu_2\text{-}OCH_2CH_2)N]\}_2$ (**1b**, right). Thermal ellipsoids are drawn at the 50% probability level, and H atoms are omitted for clarity.

Table 1. Summary of Selected Bond Lengths and Bond Angles for $Ti_2(O^iPr)_2\{[(O\text{-}2,4\text{-}Me_2C_6H_2\text{-}6\text{-}CH_2)_2(\mu_2\text{-}OCH_2CH_2)N]\}_2$ (1a) and $Ti_2(O^tBu)_2\{[(O\text{-}2,4\text{-}Me_2C_6H_2\text{-}6\text{-}CH_2)_2(\mu_2\text{-}OCH_2CH_2)N]\}_2$ (1b)

	1a	1b
	Selected Bond Distances (Å)	
Ti(1)−O(1), Ti(1)−O(2)	1.922(2), 1.872(3)	1.896(2), 1.934(2)
Ti(2)−O(5), Ti(2)−O(6)	1.892(2), 1.855(2)	1.903(2), 1.873(2)
Ti(1)−O(3), Ti(2)−O(3)	2.056(2), 2.001(2)	2.046(2), 2.007(2)
Ti(1)−O(7), Ti(2)−O(7)	1.986(2), 2.081(2)	1.972(2), 2.094(2)
Ti(1)−O(4), Ti(2)−O(8)	1.812(2), 1.778(3)	1.776(2), 1.751(3)
Ti(1)−N(1), Ti(2)−N(2)	2.258(3), 2.341(3)	2.278(3), 2.327(3)
	Selected Bond Angles (deg)	
O(1)−Ti(1)−O(2), O(5)−Ti(2)−O(6)	160.24(11), 102.97(12)	161.46(11), 104.10(10)
O(7)−Ti(1)−N(1), O(7)−Ti(2)−N(2)	147.64(10), 75.00(11)	149.47(9), 75.83(9)
O(3)−Ti(1)−O(4), O(3)−Ti(2)−O(8)	172.40(12), 92.61(13)	172.10(12), 93.96(11)
O(3)−Ti(1)−O(7), O(3)−Ti(2)−O(7)	72.63(9), 71.78(9)	72.80(8), 71.08(8)
Ti(1)−O(3)−Ti(2), Ti(1)−O(7)−Ti(2)	107.55(11), 107.18(11)	106.40(10), 105.89(10)
O(1)−Ti(1)−O(3), O(7)−Ti(2)−O(8)	90.24(11), 104.58(13)	94.18(10), 104.65(10)
Ti(1)−O(1)−C(1), Ti(1)−O(2)−C(10)	122.4(2), 134.9(2)	124.4(2),132.1(2)
Ti(2)−O(5)−C(24), Ti(2)−O(6)−C(33)	142.9(2), 135.3(2)	139.9(2), 140.3(2)[a]
Ti(1)−O(4)−C(21), Ti(2)−O(8)−C(44)	142.6(3), 156.3(4)	170.7(2), 171.3(2)[b]

[a] Ti(2)−O(6)−C(34). [b] Ti(2)−O(8)−C(45).

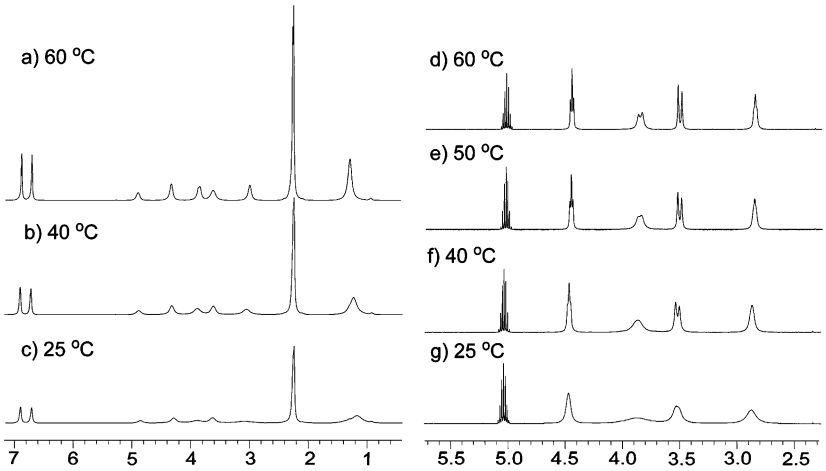

Figure 2. Variable-temperature ^1H NMR spectra (in $CDCl_3$) of **1a** (left) and **1b** (right, expanded chart from 2.5 to 5.0 ppm).

distorted trigonal bipyramidal structure around Ti consisting of a plane composed of two aryloxo and one alkoxo ligand and an N−Ti−O (in O^{t}Bu) axis as evident from the O−Ti−N bond angle [O(4)−Ti(1)−N(1) 176.01(8)°]. No distinct differences in the bond distances and the angles are seen between **2a** and **2b** (Table 2).

Figure 4 shows ^1H NMR spectra (in $CDCl_3$) for **2a** and **2b**. Relatively sharp resonances compared to **1a** were observed even

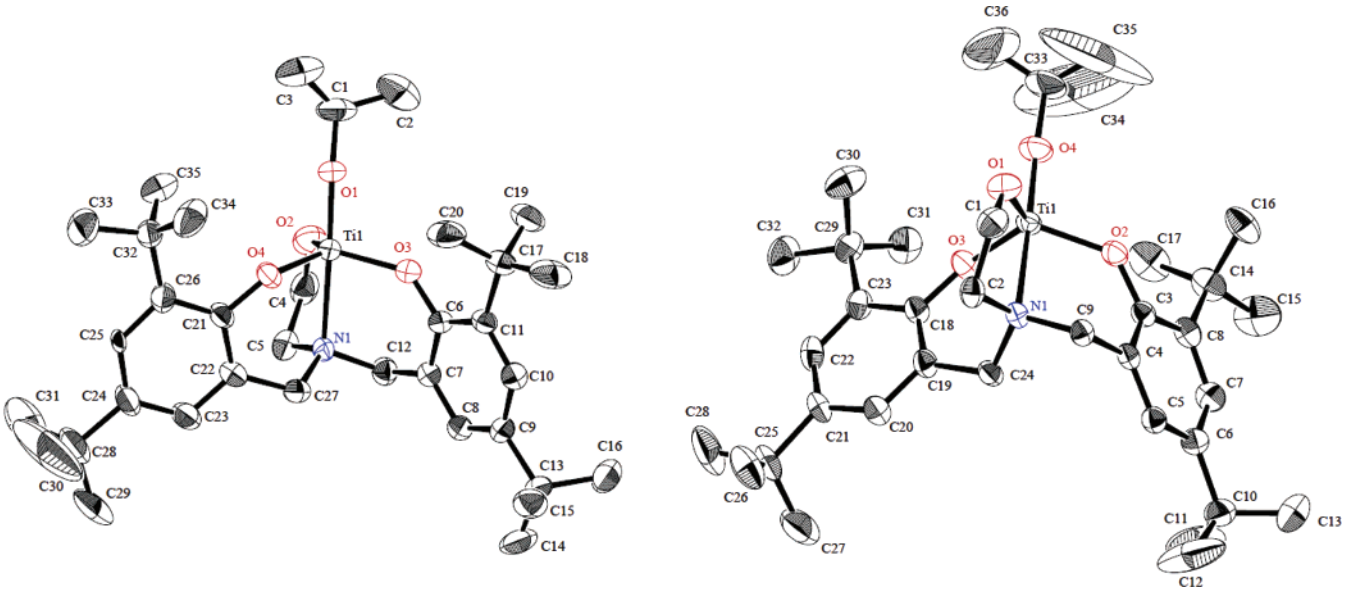

Figure 3. ORTEP drawings for Ti(O^{i}Pr)[(O-2,4-^{t}Bu$_2$C$_6$H$_2$-6-CH$_2$)$_2$(OCH$_2$CH$_2$)N] (**2a**, right) and Ti(O^{t}Bu)[(O-2,4-^{t}Bu$_2$C$_6$H$_2$-6-CH$_2$)$_2$(OCH$_2$CH$_2$)N] (**2b**). Thermal ellipsoids are drawn at the 50% probability level, and H atoms are omitted for clarity.

Table 2. Summary of Selected Bond Lengths and Bond Angles for Ti(O^{i}Pr)[(O-2,4-^{t}Bu$_2$C$_6$H$_2$-6-CH$_2$)$_2$(OCH$_2$CH$_2$)N] (2a) and Ti(O^{t}Bu)[(O-2,4-^{t}Bu$_2$C$_6$H$_2$-6-CH$_2$)$_2$(OCH$_2$CH$_2$)N] (2b)

	Selected Bond Distances (Å) for **2a**	
Ti(1)−O(1) 1.770(3)	Ti(1)−O(2) 1.825(4)	Ti(1)−O(3) 1.854(3)
Ti(1)−O(4) 1.838(3)	Ti(1)−N(1) 2.328(3)	
	Selected Bond Distances (Å) for **2b**	
Ti(1)−O(1) 1.8390(17)	Ti(1)−O(2) 1.8689(16)	Ti(1)−O(3) 1.842(2)
Ti(1)−O(4) 1.772(2)	Ti(1)−N(1) 2.328(2)	
	Selected Bond Angles (deg) for **2a**	
O(1)−Ti(1)−O(2) 96.65(18)	O(1)−Ti(1)−O(3) 99.50(14)	O(1)−Ti(1)−N(1) 174.14(19)
O(2)−Ti(1)−O(3) 118.80(17)	O(2)−Ti(1)−O(4) 117.12(17)	O(2)−Ti(1)−N(1) 77.49(15)
Ti(1)−O(1)−C(1) 151.9(5)	Ti(1)−O(2)−C(4) 125.3(3)	Ti(1)−O(3)−C(6) 138.8(2)
Ti(1)−O(4)−C(21) 137.7(3)	Ti(1)−N(1)−C(5) 103.7(2)	
	Selected Bond Angles (deg) for **2b**	
O(1)−Ti(1)−O(4) 98.56(10)	O(2)−Ti(1)−O(4) 98.89(8)	O(4)−Ti(1)−N(1) 176.01(8)
O(3)−Ti(1)−O(4) 99.77(10)	O(1)−Ti(1)−O(2) 118.21(9)	O(1)−Ti(1)−N(1) 77.45(8)
Ti(1)−O(4)−C(33) 166.4(2)	Ti(1)−O(1)−C(1) 125.30(19)	Ti(1)−O(2)−C(3) 134.98(14)
Ti(1)−O(3)−C(18) 142.07(16)	Ti(1)−N(1)−C(2) 103.14(15)	

at 25 °C in the ^{1}H NMR spectra for **2a** (Figure 4d vs Figure 2c); each resonance corresponded to methylene protons, which were slightly improved at higher temperature. Although the ^{1}H NMR spectra for **2a** were rather sharp compared to **1a**, the ^{1}H NMR spectra of **2b** (Figure 4e−h) showed broad resonances at 25 °C (Figure 2g); each resonance of **2b** became sharp at 60 °C (Figure 4h). Although the monomeric nature of compound **2b** could be confirmed by X-ray crystallography, the ^{1}H NMR signals for the CH_2 and CH_3 protons were still broad.

As described above, the observed broad resonances/temperature dependences might be due to several reasons such as (1) the cleavage of poly- or oligonuclear into monomeric species, (2) equilibrium between dimeric and monomeric species, and (3) the fluxional natures of the methylene units in these ligands. The latter explanation may be most probable considering the ^{1}H NMR spectra of the monomeric titanatranes, because similar temperature dependences were seen even in the spectra for the monomeric species.

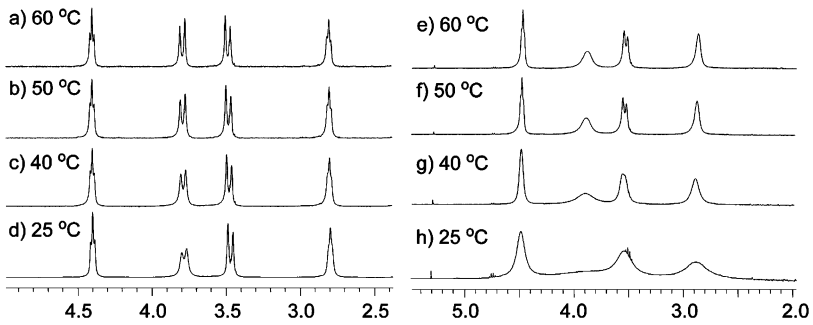

Figure 4. Variable-temperature ^{1}H NMR spectra (in $CDCl_3$, expanded from 2.5 to 5.5 ppm) for **2a** (left) and **2b** (right).

Scheme 2

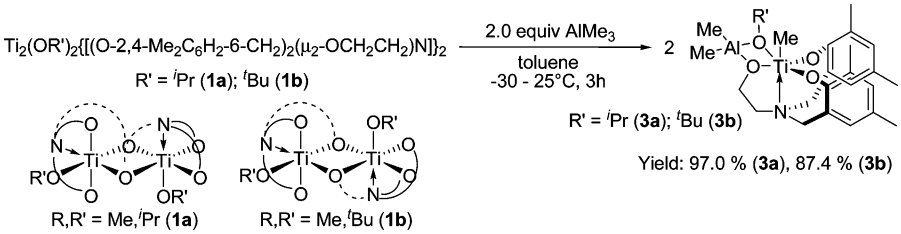

Reactions of $Ti_2(OR')_2\{[(O\text{-}2,4\text{-}Me_2C_6H_2\text{-}6\text{-}CH_2)_2(\mu_2\text{-}OCH_2CH_2)N]\}_2$ (1a, 1b) with $AlMe_3$. Isolation and Structural Determinations of $\{TiMe[(O\text{-}2,4\text{-}Me_2C_6H_2\text{-}6\text{-}CH_2)_2(\mu_2\text{-}OCH_2CH_2)N]\}[Me_2Al(\mu_2\text{-}OR')]$ (3a, 3b) Complexes. We communicated that the titanium complexes containing tris(aryloxo)amine ligands of the type $[TiX\{(O\text{-}2,4\text{-}R_2C_6H_2\text{-}6\text{-}CH_2)_3N\}]$ (R = Me, ^{t}Bu; X = O^{i}Pr, O-2,6-^{i}Pr$_2$C$_6$H$_3$) exhibited notable catalytic activities for ethylene polymerization in the presence of MAO, especially at 100−120 °C.[10] The activities increased upon the addition of a small amount of $AlMe_3$, and the activities decreased upon further addition. We assumed that the selective cleavage of one of three Ti−O bonds would afford the catalytically active cationic alkyl−Ti species in the presence MAO. In order to explore the possibility of cleavage of the Ti−O bond by reaction of $AlMe_3$, reactions of **1a** and **1b** with $AlMe_3$ were performed.[24] Titanatranes containing bis(aryloxo)-(alkoxo)amine ligands were chosen, because cleavage of alkoxo rather than arloxo ligands containing substituents in the *ortho* position was considered. Moreover, as presented below, we assumed that the formed species may be active as catalytically active species for olefin polymerization even in the absence of MAO.

The reaction of $Ti_2(O^iPr)_2\{[(O\text{-}2,4\text{-}Me_2C_6H_2\text{-}6\text{-}CH_2)_2(OCH_2\text{-}CH_2)N]\}_2$ (**1a**) with 2.0 equiv of $AlMe_3$ (1.0 equiv to Ti) in toluene gave a Ti−Me complex coordinated to $Me_2Al(O^iPr)$, $\{TiMe[(O\text{-}2,4\text{-}Me_2C_6H_2\text{-}6\text{-}CH_2)_2(\mu_2\text{-}OCH_2CH_2)N]\}[Me_2Al(\mu_2\text{-}O^iPr)]$ (**3a**), in exclusive yield (97.0%, Scheme 2). **3a** could be identified by ^{1}H and ^{13}C NMR spectra and elemental analysis as well as X-ray crystallography (Figure 5, left). ^{1}H NMR spectra (in $CDCl_3$) showed sharp resonances assignable to **3a**, and no distinct differences in the spectra were seen between 25 and 55 °C, suggesting formation of the monomeric compound. The new resonances observed at ca. −0.8 and 1.1 ppm in the ratio of 2:1 (6:3) clearly indicate the formation of a new heterobimetallic complex containing TiMe and $AlMe_2$ groups.

The crystallographic analysis reveals that **3a** has a rather distorted octahedral geometry around Ti, consisting of a C (in Me)−Ti−N axis [N(1)−Ti(1)−C(1) 171.82(7)°] and a distorted plane of two aryloxo and two alkoxo ligands (Table 3). Although the cleavage of the Ti−O^{i}Pr bond can be confirmed from the bond distance of the Ti−O^{i}Pr in **1a** and **3a** [1.778(3), 1.812(2) Å in **1a** vs 2.0594(12) Å in **3a**] affording the Ti−Me complex by replacement of Ti−O^{i}Pr in **1a** with $AlMe_3$, oxygen in the O^{i}Pr still coordinates to Ti; no significant differences in the Ti−O bond distances between the Ti−O (O^{i}Pr) and Ti−O are seen (alkoxo in the ligand) [Ti(1)−O(1), Ti(1)−O(2) 2.0594-(12), 2.0453(11) Å, respectively], and these O atoms are coordinated to both Ti and Al. The Ti−N bond distance [2.4171-(16) Å] is somewhat longer than those in **1a** [2.258(3), 2.341-(3) Å]. **3a** was found to be very stable as microcrystals and could be stored for long periods in the drybox without partial decomposition. Rapid decomposition could not be seen even after exposure of **3a** to the atmosphere; this is contrary to many Ti−methyl and Al−methyl compounds. However, a mixture of **3a** and unidentified compounds was seen if **3a** was stored in chlorinated solvents for many hours.

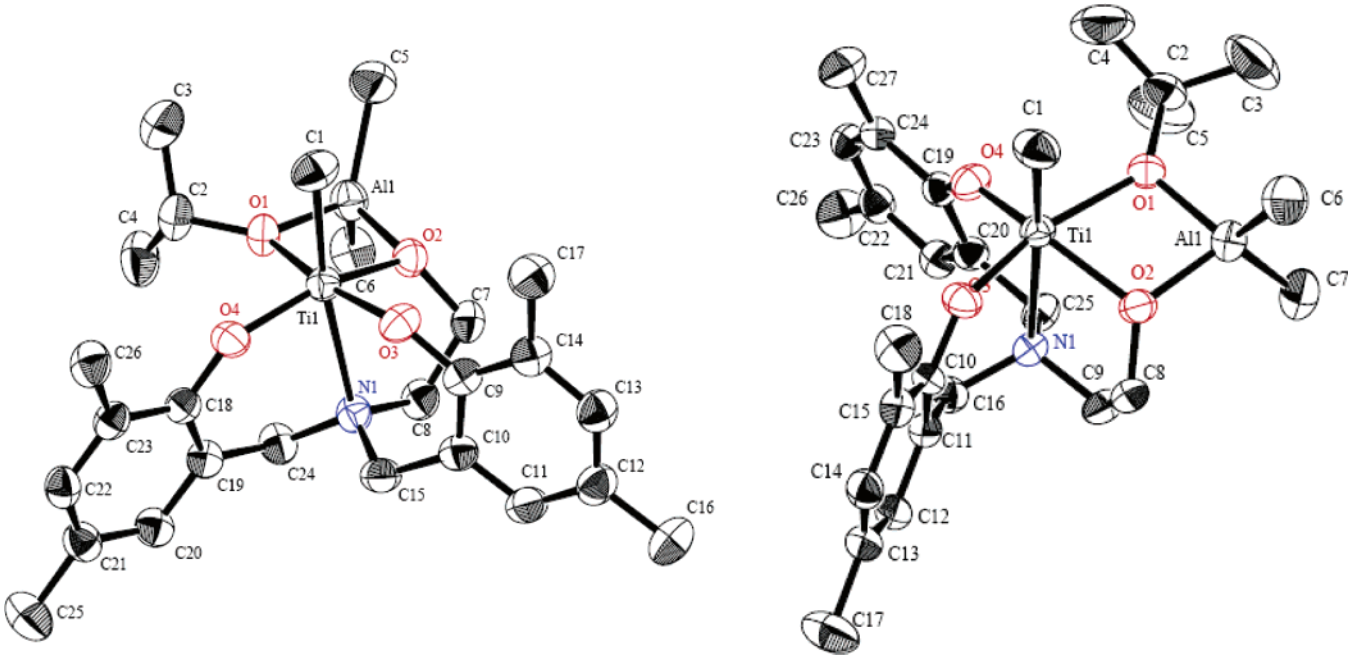

Figure 5. ORTEP drawings for $\{TiMe[(O\text{-}2,4\text{-}Me_2C_6H_2\text{-}6\text{-}CH_2)_2(\mu_2\text{-}OCH_2CH_2)N]\}[Me_2Al(\mu_2\text{-}O^iPr)]$ (**3a**, left) and $\{TiMe[(O\text{-}2,4\text{-}Me_2C_6H_2\text{-}6\text{-}CH_2)_2(\mu_2\text{-}OCH_2CH_2)N]\}[Me_2Al(\mu_2\text{-}O^tBu)]$ (**3b**, right). Thermal ellipsoids are drawn at the 50% probability level, and H atoms are omitted for clarity.

Table 3. Summary of Selected Bond Length and Bond Angles for {TiMe[(O-2,4-$Me_2C_6H_2$-6-CH_2)$_2$(μ_2-OCH_2CH_2)N]}[Me_2Al(μ_2-O^{i}Pr)] (3a) and {TiMe[(O-2,4-$Me_2C_6H_2$-6-CH_2)$_2$(μ_2-OCH_2CH_2)N]}[Me_2Al(μ_2-O^{t}Bu)] (3b)

	3a	3b
	Selected Bond Distances (Å)	
Ti(1)−C(1), Ti(1)−N(1)	2.103(2), 2.4171(16)	2.117(3), 2.454(2)
Ti(1)−O(1), Ti(1)−O(2)	2.0594(12), 2.0453(11)	2.086(2), 2.024(2)
Ti(1)−O(3), Ti(1)−O(4)	1.8392(13), 1.8281(12)	1.837(2), 1.821(2)
Al(1)−O(1), Al(1)−O(2)	1.8303(12), 1.8366(14)	1.834(2), 1.825(2)
Al(1)−C(5), Al(1)−C(6)	1.958(2), 1.962(2)	1.953(4), 1.956(4)[a]
	Selected Bond Angles (deg)	
O(1)−Ti(1)−O(2), O(1)−Al(1)−O(2)	72.03(4), 82.32(5)	71.97(9), 82.62(11)
O(1)−Ti(1)−O(3), O(2)−Ti(1)−O(4)	166.20(5), 149.25(5)	164.98(10), 147.87(9)
O(1)−Ti(1)−O(4), O(2)−Ti(1)−O(3)	90.99(5), 94.18(5)	93.11(10), 93.49(10)
N(1)−Ti(1)−C(1)	171.82(7)	167.50(13)
C(5)−Al(1)−C(6)	115.81(10)	117.66(18)[b]
Ti(1)−O(1)−Al(1), Ti(1)−O(2)−Al(1)	101.97(6),102.28(6)	100.82(11), 103.48(11)
Ti(1)−O(3)−C(9), Ti(1)−O(4)−C(18)	142.93(12), 142.92(11)	146.9(2), 144.96(19)[c]
Ti(1)−O(1)−C(2), Al(1)−O(1)−C(2)	126.72(10), 129.96(11)	135.4(2), 123.4(2)

[a] Al(1)−C(6), Al(1)−C(7), respectively. [b] C(6)−Al(1)−C(7). [c] Ti(1)−O(3)−C(10), Ti(1)−O(4)−C(19), respectively.

The reaction of **1b** with 2.0 equiv of $AlMe_3$ (1.0 equiv to Ti) cleanly afforded another heterobimetallic Ti−Me complex (**3b**) in high yield (89.4%). **3b** was identified by ^{1}H and ^{13}C NMR spectra and elemental analysis, and the structure could be determined by X-ray crystallography.

The crystallographic analysis for **3b** (Table 3, right) reveals that the basic structure of **3b** was analogous to **3a**; **3b** has a distorted octahedral geometry around Ti, consisting of a C (in Me)−Ti−N axis [N(1)−Ti(1)−C(1) 167.50(13)°] and a rather distorted plane formed by two aryloxo and two alkoxo ligands (Figure 3, right). The N−Ti−C bond angle is somewhat smaller than that in **3a** [171.82(7)°], probably due to the steric bulk of the O^{t}Bu group (positioned close to Me). The Ti−N bond distance in **3b** [2.454(2) Å] is also longer than that in **3a** [2.4171(16)] and **1a**,**b** and **2a**,**b** [2.258−2.341 Å], suggesting that the N atom is coordinated weakly to Ti. No remarkable differences are seen in the other bond distances and angles.

The assumption of possible cleavage of the third arm of the ligand by MAO to give way for the monomer incorporation was already reported by Eisen[26] for the stereoregular polymerization of α-olefins using C_3 symmetric group 4 benzamidinate complexes. These complexes are active catalyst for propylene polymerization to afford elastomeric polypropylene and for the syndiospecific styrene polymerization. In the presence of MAO, one of the benzamidinate ligands was displaced proceeding most likely through a η^3 to η^1 slippage mechanism; that is, one of the benzamidinate ligands dissociates and creates the required vacant space for the monomer to coordinate. Sundararajan et al. proposed a similar mechanism for the sterically and electronically modified tris(ethanol)amine-based titanium catalysts for ethylene polymerization in the presence of MAO.[17b] As far as we know, there are no reports showing the *direct* cleavage of an alkoxide ligand or alkoxide arm by Al alkyls, and these are thus the unique first examples for isolation of heterobimetallic complexes containing both Ti−Me and Al−Me bonds.

Polymerization of Ethylene. Dimeric titanatrane (**1a**) and monomeric titanatrane (**2b**) were chosen to evaluate their ability as catalyst precursors for ethylene polymerization in the presence of MAO, and the results are summarized in Table 4. These complexes exhibited moderate catalytic activities for ethylene polymerization, and the activities increased especially at high temperature (100−120 °C). The activities in octane were higher than those in toluene,[27] and the activities in octane did not decrease after 60 min (runs 4−7, 15, 16). The catalytic activities further increased upon addition of a small amount of $AlMe_3$, as seen in the polymerization using titanium complexes containing tris(aryloxo)amine ligands.[16] High catalytic activity at high polymerization temperature is promising especially from the engineering aspect, because the solution polymerization process at high temperature improves viscosity in the reaction mixture, leading to better mass transportation as well as temperature control. However, the observed catalytic activities were lower than those observed in the polymerization using Ti(O^{i}Pr)[(O-2,4-$Me_2C_6H_2$-6-CH_2)$_3$N] under the same conditions (e.g., 2290 kg PE/mol Ti·h at 120 °C in octane as run 4, 3550 kg PE/mol Ti·h upon addition of 10 equiv of $AlMe_3$ as run 6).[16] The resultant polymers prepared by the **1a**−MAO catalyst were linear polyethylene (PE), confirmed by ^{13}C NMR spectra and possessing relatively high molecular weights with unimodal molecular weight distributions in most cases. The M_w values for the resultant PEs prepared by **1a** were higher than those by **2b** due to the steric effect of the substituent on the aryloxo ligand (methyl in **1a** vs ^{t}Bu in **2b**). The molecular weight distributions for resultant PEs prepared in the presence of $AlMe_3$ were bimodal, although the reason is not clear at this moment.

The results for ethylene polymerization by **3a** and **3b** are summarized in Table 5. Both **3a** and **3b** exhibited moderate catalytic activities in the presence of MAO (runs 22−28), affording high molecular weight linear PEs confirmed by ^{13}C NMR spectra with unimodal molecular weight distributions. Note that both the catalytic activities and M_w values (for ethylene polymerization by **3a**,**b** in the presence of MAO) were similar to those by **1a** in the presence of $AlMe_3$/MAO. These results suggest that **3a** should be first formed in the reaction mixture for the ethylene polymerization by **1a** in the presence of both MAO and a small amount of $AlMe_3$ (runs 7, 14), and the efficient formation of **3a** should be responsible for exhibiting the higher catalytic activity (especially in the presence of $AlMe_3$).

(26) Averbuj, C.; Tish, E.; Eisen, M. S. *J. Am. Chem. Soc*. **1998**, *120*, 8640−8646.

(27) We assume that there are two possibilities for explaining the lower catalytic activities in toluene for ethylene polymerization such as (1) a difference (solvent effect) in the equilibrium for generating the catalytically active species shown in Scheme 3 and (2) coordination of toluene toward the catalytically active species (leading to the deactivation eventually). For a leading reference on coordination of toluene toward catalytically active species: Scollard, J. D.; McConville, D. H.; Payne, N. C; Vittal, J. J. *Macromolecules* **1996**, *29*, 5241−5243.

Table 4. Polymerization of Ethylene Using 1a and 2b Cocatalyst Systems[a]

run	complex (μmol)	cocatalyst (Al/Ti)[b] MAO/$AlMe_3$	solvent	temp/°C	time/min	yield/mg	activity[c]	M_w[d] $\times 10^{-4}$	M_w/M_n[d]
1	**1a** (1.0)	3000/−	octane	80	60	150	150	27.2	2.50
2	**1a** (1.0)	3000/−	octane	100	60	149	149	52.9	2.89
3	**1a** (10.0)	500/−	octane	120	60	1160	116	12.2	2.18
4	**1a** (1.0)	3000/−	octane	120	60	165	165	25.5	2.52
5	**1a** (1.0)	3000/−	octane	120	10	24	144	18.8	2.45
6	**1a** (1.0)	3000/10	octane	120	60	355	355	14.1	bimodal
7	**1a** (1.0)	3000/10	octane	120	10	60	360	19.0	3.18
8	**1a** (1.0)	3000/−	toluene	60	60	22	22	67.0	bimodal
9	**1a** (1.0)	3000/−	toluene	80	60	42	42	42.8	bimodal
10	**1a**(10.0)	500/−	toluene	100	60	540	54	4.09	4.01
11	**1a** (1.0)	3000/−	toluene	100	60	83	83	24.5	2.45
12	**1a** (1.0)	3000/−	toluene	100	10	21	126	26.0	2.01
13	**1a** (1.0)	3000/10	toluene	100	60	172	172	19.0	bimodal
14	**1a** (1.0)	3000/10	toluene	100	10	45	270	16.7	bimodal
15	**2b** (1.0)	3000/−	octane	120	60	220	220	0.71	2.32
16	**2b** (1.0)	3000/−	octane	120	10	28	168	0.21	2.39
17	**2b** (1.0)	3000/−	octane	100	60	205	205	3.98	bimodal
18	**2b** (1.0)	3000/10	octane	120	10	62	372	1.00	bimodal
19	**2b** (1.0)	3000/−	toluene	100	10	22	132	0.25	3.80
20	**2b** (1.0)	3000/−	toluene	100	60	218	218	0.31	2.61
21	**2b** (1.0)	3000/10	toluene	100	10	41	246	8.70	bimodal

[a] Reaction conditions: solvent (30 mL), ethylene 8 atm, 100 mL scale autoclave, d-MAO (prepared by removing $AlMe_3$ and toluene from commercially available MAO). [b] Molar ratio of Al/Ti. [c] Activity = kg PE/mol Ti·h. [d] GPC data in *o*-dichlorobenzene versus polystyrene standards.

Table 5. Polymerization of Ethylene by 3a and 3b[a]

run	complex (μ mol)	MAO Al/Ti[b]	solvent	temp/°C	time/min	yield/mg	activity[c]/ kg PE/mol Ti·h	M_w[d] $\times 10^{-4}$	M_w/M_n[d]
22	**3a** (1.0)	3000	octane	120	10	80	480	16.7	2.48
23	**3a** (1.0)	3000	octane	120	60	351	351		
7	**1a** (1.0)	3000[e]	octane	120	10	60	360	19.0	3.18
24	**3a** (1.0)	3000	toluene	100	60	292	292	21.1	2.41
25	**3a** (1.0)	3000	toluene	100	10	45	270	18.5	3.24
14	**1a** (1.0)	3000[e]	toluene	100	10	45	270	16.7	bimodal
26	**3b** (1.0)	3000	octane	120	60	302	302		
18	**2b** (1.0)	3000[e]	octane	120	10	62	372	1.00	bimodal
27	**3b** (1.0)	3000	toluene	100	10	50	300	7.90	3.07
28	**3b** (1.0)	3000	toluene	100	60	182	182	22.3	2.58
29	**3a** (1.0)		octane	120	60	trace[f]			
30	**3a** (1.0)		toluene	100	60	trace[f]			
31	**3b** (1.0)		octane	120	60	94	94	100.2	2.58
32	**3b** (1.0)		octane	120	60	87	87		
33	**3b** (1.0)		toluene	100	60	trace[g]			

[a] Reaction conditions: solvent (30 mL), ethylene 8 atm, 100 mL scale autoclave, d-MAO (prepared by removing $AlMe_3$ and toluene from commercially available MAO). [b] Molar ratio of Al/Ti (MAO 3.0 mmol). [c] Activity = kg PE/mol Ti·h. [d] GPC data in *o*-dichlorobenzene versus polystyrene standards. [e] Addition of 10 equiv of $AlMe_3$ (shown in Table 4). [f] Negligible amount of polymer was formed. [g] Trace amount of polyethylene (ca. <15 mg) could be collected.

It is important to note that ***3b** exhibited moderate catalytic activity for ethylene polymerization in octane without MAO, affording high molecular weight PE with uniform molecular weight distribution* (run 31, activity 94 kg PE/mol Ti·h, $M_w = 1.00 \times 10^6$, $M_w/M_n = 2.58$). The result using **3b** without MAO was reproducible (run 32), and a trace amount of polyethylene (<15 mg) was collected if the polymerization was performed in toluene at 100 °C. However, **3a** showed negligible catalytic activity under the same conditions in octane, and the activity in toluene was also negligible.[27] Although the effect of alkoxide ligand on Al on the activity is critical, the results suggest that ethylene polymerization took place by cleavage of Ti−O bonds, as shown in Scheme 3, and the cationic species (**4** in Scheme 3) plays a key role as the catalytically active species for ethylene polymerization, as assumed in the previous communication.[16] It may also be assumed that the equilibrium is sensitive to the steric bulk on the alkoxide ligand on Al; therefore, ethylene polymerization by less bulky **3a** (OR′ = O^{i}Pr) than **3b** (OR′ = O^{t}Bu) showed negligible catalytic activity under the same conditions. The fact that the M_w value for the resultant PE by **3b** (without additional cocatalyst) was much higher than those for the PEs prepared by **3b**−MAO catalyst also suggests that chain transfer to Al accompanied the ethylene polymerization in the presence of MAO.

Concluding Remarks

We have prepared dimeric titanatranes $Ti_2(OR')_2\{[(O\text{-}2,4\text{-}Me_2C_6H_2\text{-}6\text{-}CH_2)_2(\mu_2\text{-}OCH_2CH_2)]N\}_2$ [R′ = ^{i}Pr (**1a**), ^{t}Bu (**1b**)] and the monomeric titanatranes $Ti(OR')[(O\text{-}2,4\text{-}^tBu_2C_6H_2\text{-}6\text{-}CH_2)_2(OCH_2CH_2)]N$ (**2a**,**b**) in high yields by the reaction of $Ti(OR')_4$ with $[(HO\text{-}2,4\text{-}R_2C_6H_2\text{-}6\text{-}CH_2)_2(HOCH_2CH_2)]N$ (R = Me, ^{t}Bu) in toluene. The reaction of **1a**,**b** with 2.0 equiv of $AlMe_3$ in toluene gave the Ti−Me complexes coordinated to $Me_2Al(OR')$ of type $\{TiMe[(O\text{-}2,4\text{-}Me_2C_6H_2\text{-}6\text{-}CH_2)_2(\mu_2\text{-}OCH_2\text{-}CH_2)N]\}[Me_2Al(\mu_2\text{-}OR')]$ [R′ = ^{i}Pr (**3a**), ^{t}Bu (**3b**)], in exclusive yields, and these complexes were identified by ^{1}H and ^{13}C NMR spectra, elemental analyses, and X-ray crystallography. Complexes **1a** and **2b** exhibited moderate catalytic activities for ethylene polymerization at 100−120 °C in the presence of MAO, and the activity increased upon the presence of a small amount of $AlMe_3$. Similar catalytic activities were observed if

Scheme 3

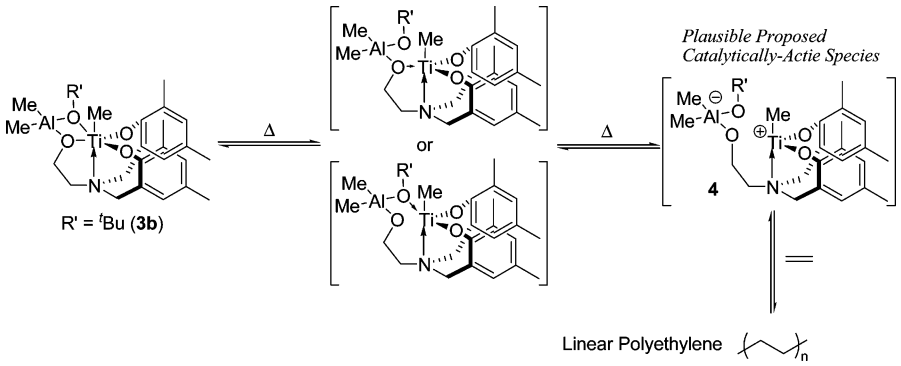

3a,**b** were used in the presence of MAO, affording high molecular weight polyethylene with unimodal molecular weight distributions. The activities and M_w values of **3a**,**b** in the presence of MAO were similar to those of **1a** in the presence of $AlMe_3$/MAO.

Ethylene polymerization in octane by **3b** took place without additional cocatalyst with moderate catalytic activity (94 kg PE/mol Ti·h), affording high molecular weight polymer with unimodal distribution. Although the effect of the alkoxide ligand on Al toward the catalytic activity is critical, the results clearly suggest that the ethylene polymerization took place by cleavage of Ti−O bonds, as shown in Scheme 3, and the cationic species (**4**) plays a key role as the catalytically active species for ethylene polymerization. We believe that the present catalysis introduces new promising concept for the catalyst design directed toward precise olefin polymerization; studying the effect of substituents and the alkoxo and aryloxo ligands is still under way, and the results will be introduced in the near future.

Experimental Section

General Procedures. All experiments were carried out under a nitrogen atmosphere in a Vacuum Atmospheres drybox or by using standard Schlenk techniques unless otherwise specified. All chemicals used were of reagent grade and were purified by the standard purification procedures. Toluene (anhydrous grade, Kanto Kagaku Co., Ltd.) and *n*-octane (anhydrous grade, Aldrich) for polymerization were stored in a bottle in the drybox in the presence of molecular sieves. Ethylene was of polymerization grade (purity >99.9%, Sumitomo Seika Co. Ltd) and was used as received. Toluene and $AlMe_3$ in the commercially available methylaluminoxane [PMAO-S, 9.5 wt % (Al) toluene solution, Tosoh Finechem Co.] were taken to dryness under reduced pressure (at ca. 50 °C for removing toluene and $AlMe_3$ and then heated at >100 °C for 1 h for completion) in the drybox to give white solids. Bis(2-hydroxy-3,5-dimethylbenzyl)ethanolamine (**Lig 1**) and bis(2-hydroxy-3,5-di-*tert*-butylbenzyl)ethanolamine (**Lig 2**) were prepared according to a previous report.[28] Molecular weights and molecular weight distributions for polyethylene were measured by gel permeation chromatography (Tosoh HLC- 8121GPC/HT) with a polystyrene gel column (TSK gel GMHHR-H HT × 2, 30 cm × 7.8 mm ϕ i.d.), ranging from $<10^2$ to $<2.8 \times 10^8$ MW) at 140 °C using *o*-dichlorobenzene containing 0.05 w/v % 2,6-di-*tert*-butyl-*p*-cresol as eluent. The molecular weight was calculated by a standard procedure based on the calibration with standard polystyrene samples.

All ^{1}H and ^{13}C NMR spectra were recorded on a JEOL JNM-LA 400 spectrometer (399.65 MHz, ^{1}H). All deuterated NMR solvents were stored over molecular sieves under a nitrogen atmosphere in the drybox, and all chemical shifts are given in ppm and are referenced to Me_4Si. All spectra were obtained in the solvent indicated at 25 °C unless otherwise noted. ^{13}C NMR spectra for polyethylene were recorded on a JEOL JNM-LA400 spectrometer (100.40 MHz, ^{13}C) with proton decoupling. The pulse interval was 5.2 s, the acquisition time was 0.8 s, the pulse angle was 90°, and the analysis samples were prepared by dissolving polymers in a mixed solution of 1,2,4-trichlorobenzene/benzene-d_6 (90/10 wt); these spectra were measured at 110 °C.

Synthesis of $Ti_2(O^iPr)_2${[(O-2,4-$Me_2C_6H_2$-6-CH_2)$_2$(μ_2-OCH_2-CH_2)N]}$_2$ (1a). Bis(2-hydroxy-3,5-dimethylbenzyl)ethanolamine, (HO-2,4-$Me_2C_6H_2$-6-CH_2)$_2$($HOCH_2CH_2$)N (**Lig 1**, 0.411 g, 1.25 mmol), in toluene (10 mL) was added dropwise into a toluene solution (10 mL) containing $Ti(O^iPr)_4$ (0.355 g, 1.25 mmol) at −30 °C. The reaction mixture was then stirred at room temperature for 6 h, and the volatiles were then evaporated under vacuum, leaving an orange-yellow solid. The resultant solids were dissolved with 15 mL of toluene, and the orange solution was filtered through a Celite pad and placed in the freezer (−30 °C). The desired product **1a** was isolated as yellow microcrystals from the chilled toluene solution. Yield: 0.466 g (86.0%). Nature: Pale yellow, crystalline solid. ^{1}H NMR ($CDCl_3$, 25 °C): δ 1.33 (br s, 6H, $C(CH_3)_2$), 2.01 (br s, 12H, Ar−CH_3), 2.87 (br s, 2H, N−CH_2), 3.53 (br s, 2H, CH_2−Ar), 3.81 (br s, 2H, CH_2−Ar), 4.35 (br s, 2H, O−CH_2), 4.88 (br s, 1H, CH), 6.70 (br s, 2H, Ar−H), 6.86 (br s, 2H, Ar−H). ^{1}H NMR ($CDCl_3$, 55 °C): the resonances became sharp, but we could not see the multiplicities of these signals and there is no change in the chemical shift for all protons (Figure 2). ^{13}C NMR ($CDCl_3$, 25 °C): δ 14.10 (CH(CH_3)$_2$), 20.52 (Ar−CH_3), 25.43 (Ar−CH_3), 57.14 (N−CH_2), 59.97 (br, Ar−CH_2), 70.25 (O−CH_2), 78.54 (*C*H), 123.26, 124.67, 127.20, 130.74, 158.53. Anal. Calcd for $C_{46}H_{62}N_2O_8Ti_2$: C, 63.74 or 62.36(+TiC); H, 7.21; N, 3.23. Found: C, 62.64; H, 7.44; N, 3.07.

Synthesis of $Ti_2(O^tBu)_2${[(O-2,4-$Me_2C_6H_2$-6-CH_2)$_2$(μ_2-OCH_2-CH_2)N]}$_2$ (1b). Compound **1b** was prepared according to a procedure analogous to that given for **1a**, except **Lig 1** (0.343 g, 1.0 mmol) and $Ti(O^tBu)_4$ (0.340 g, 1.0 mmol) were used. Nature: Pale yellow, crystalline solid. Yield: 0.366 g (81.8%). ^{1}H NMR ($CDCl_3$, 25 °C): δ 1.55 (s, 9H), 2.20 (br s, 12H), 2.80 (t, 2H, N−CH_2), 3.48 (d, J = 12 Hz, 2H, CH_2Ar), 3.79 (d, J = 12 Hz, 2H, CH_2Ar), 4.40 (t, 2H, O−CH_2), 6.71 (s, 2H, Ar−H), 6.87 (s, 2H, Ar−H). ^{13}C NMR ($CDCl_3$, 25 °C): δ 14.11 (C(CH_3)$_3$), 20.51 (Ar−CH_3), 31.47 (Ar−CH_3), 56.14 (N−CH_2), 56.98 (Ar−CH_2), 70.59 (O-CH_2), 84.21 ($C(CH_3)_3$), 123.08, 124.93, 127.68, 128.75, 130.84, 159.00. Anal. Calcd for $C_{24}H_{33}NO_4Ti$: C, 64.43; H, 7.43; N, 3.13. Found: C, 64.55; H, 7.51; N, 2.84.

(28) Siegl, W. O.; Chattha, M. S. Eur. Pat. Appl. 276073, 1988. The desired compounds (**Lig 1**,**2**) could be purified by recrystallization from a concentrated chilled hexane solution (−50 °C). The resultant white solids were dissolved in hexane and passed through a short alumina column under N_2 in the drybox. White microcrystals were then collected from the chilled hexane solution (−25 °C). This purification procedure is important to obtain the ligands in pure form.

Table 6. Crystallographic Parameters for 1a, 1b, 2a, and 2b[a]

	1a	1b	2a	2b
empirical formula	$C_{46}H_{62}N_2O_8Ti_2$	$C_{63}H_{90}N_2O_{10}Ti_2$	$C_{35}H_{55}NO_4Ti$	$C_{36}H_{57}NO_4Ti$
fw	866.80	1131.21	601.72	615.75
cryst color, habit	yellow, block	yellow, block	yellow, block	yellow, block
cryst dimens	0.42 × 0.30 × 0.24 mm	0.50 × 0.20 × 0.10 mm	0.24 × 0.20 × 0.14 mm	0.36 × 0.34 × 0.30 mm
cryst syst	monoclinic	monoclinic	monoclinic	triclinic
lattice params	a = 12.4415(5) Å b = 18.3805(5) Å c = 21.8617(7) Å β = 91.0903(14)° V = 4998.5(3) Å^3	a = 16.8463(6) Å b = 17.3301(5) Å c = 21.5182(6) Å β = 99.7390(9)° V = 6191.7(3) Å^3	a = 10.5075(5) Å b = 29.4993(13) Å c = 11.6832(8) Å β = 104.319(2)° V = 3508.9(3) Å^3	a = 10.9424(4) Å b = 12.2541(5) Å c = 15.0994(6) Å α = 98.7288(12)° β = 106.8849(10)° γ = 103.6132(13) ° V = 1829.46(12) Å^3
space group	$P2_1/n$ (#14)	$P2_1/n$ (#14)	$P2_1/c$ (#14)	$P\bar{1}$ (#2)
Z value	4	4	4	2
D_{calc}	1.152 g/cm^3	1.213 g/cm^3	1.139 g/cm^3	1.118 g/cm^3
F_{000}	1840.00	2424.00	1304.00	668.00
μ(Mo Kα)	3.671 cm^{-1}	3.143 cm^{-1}	2.789 cm^{-1}	2.689 cm^{-1}
$2\theta_{max}$	50.0°	54.9°	54.9°	54.8°
no. of reflns measd	total: 37 044; unique: 8741 (R_{int} = 0.022)	total: 56 553; unique: 14 056 (R_{int} = 0.069)	total: 33 862 unique: 7977 (R_{int} = 0.082)	total: 17 990; unique: 8270 (R_{int} = 0.017)
no. of observations ($I > 3.00(I)$)	6246	5931	2914	6782
no. of variables	621	784	425	436
residuals: R; R_w ($I > 3.00(I)$)	0.0606; 0.1084	0.0486; 0.1152	0.0588; 0.1485	0.0586; 0.1151
goodness of fit	1.004	1.008	1.002	1.002
max. shift/error	0.001	0.001	0.002	0.007

[a] Diffractometer: Rigaku RAXIS-RAPID imaging plate. Structure solution: direct methods. Refinement: full-matrix least-squares. Function minimized: $\sum w(|F_o| - |F_c|)^2$ (w = least-squares weights). Standard deviation of an observation of unit weight: $[\sum w(|F_o| - |F_c|)^2/(N_o - N_v)]^{1/2}$ (N_o = number of observations, N_v = number of variables). Radiation: Mo Kα (λ = 0.71075 Å) graphite monochromated.

Synthesis of Ti(O^{i}Pr)[(O-2,4-^{t}Bu$_2$C$_6$H$_2$-6-CH$_2$)$_2$(OCH$_2$CH$_2$)N] (2a). Compound **2a** was prepared according to a procedure analogous to that given here for **1a**, except **Lig 2** (0.621 g, 1.25 mmol) and Ti(O^{i}Pr)$_4$ (0.355 g, 1.25 mmol) were used. Nature: Pale yellow, crystalline solid. Yield: 0.616 g (82.0%). ^{1}H NMR ($CDCl_3$, 25 °C): δ 1.28 (s, C(*CH*$_3$)$_3$, 18H), 1.45 (s, C(*CH*$_3$)$_3$, 18H),1.45 (br s, CH(*CH*$_3$)$_2$, 6H), 2.88 (br s, N−*CH*$_2$), 3.53 (br s, *CH*$_2$Ar, 2H), 3.88 (br s, *CH*$_2$Ar, 2H), 4.47 (br s, O−*CH*$_2$, 2H), 5.03 (Septet, O−CH, J = 6 Hz, 1H), 6.98 (d, 2H), 7.22 (d, 2H). ^{13}C NMR ($CDCl_3$, 25 °C): δ 26.12 (C(*C*H$_3$)$_2$), 29.62 (Ar−*C*H$_3$), 31.66 (Ar−*C*H$_3$), 34.26, 35.01, 56.26 (N−*C*H$_2$), 57.62 (Ar−*C*H$_2$), 70.75 (O−*C*H$_2$), 78.77 (*HC*(CH$_3$)$_3$), 123.26, 124.70, 124.34,135.66, 141.96, 159.62. Anal. Calcd for $C_{35}H_{55}NO_4Ti$: C, 69.87; H, 9.21; N, 2.33. Found: C, 69.80; H, 9.45; N, 2.23.

Synthesis of Ti(O^{t}Bu)[(O-2,4-^{t}Bu$_2$C$_6$H$_2$-6-CH$_2$)$_2$(OCH$_2$CH$_2$)N] (2b). Compound **2b** was prepared according to a procedure analogous to that given here for **1a**, except **Lig 2** (0.497 g, 1.0 mmol) and Ti(O^{t}Bu)$_4$ (0.340 g, 1.0 mmol) were used. Nature: Pale yellow, crystalline solid. Yield: 0.495 g (80.5%). ^{1}H NMR ($CDCl_3$, 25 °C): δ 1.29 (s, 18H, ^{t}Bu), 1.46 (s, 18H, ^{t}Bu), 1.55 (s, 9H, Ar−CH$_3$), 2.88 (br s, 2H, N−CH$_2$), 3.54 (br s, 4H, N−CH$_2$−Ar), 4.48 (br s, 2H, O−CH$_2$), 6.99 (s, 2H), 7.23 (s, 2H). ^{1}H NMR ($CDCl_3$, 55 °C): 1.29 (s, 18H, ^{t}Bu), 1.45 (s, 18H, ^{t}Bu), 1.55 (s, 9H, Ar−CH$_3$), 2.86 (br s, 2H, N−CH$_2$), 3.52 (d, J = 16 Hz, 2H, N−CH$_2$−Ar), 3.87 (d, J = 16 Hz, 2H, N−CH$_2$−Ar), 4.46 (t, 2H, O−CH$_2$), 6.97, 7.23. ^{13}C NMR ($CDCl_3$, 25 °C): δ 29.66 (C(*C*H$_3$)$_3$), 31.68 (Ar−C(*C*H$_3$)$_3$), 31.91 (Ar−C(*C*H$_3$)$_3$), 34.26 (*C*(CH$_3$)$_3$), 35.05 (*C*(CH$_3$)$_3$), 56.14 (N−*C*H$_2$), 57.63 (Ar−*C*H$_2$), 70.79 (O−*C*H$_2$), 84.13 (*C*(CH$_3$)$_3$), 123.20, 123.75, 124.31, 135.61, 141.79, 159.66. Anal. Calcd for $C_{36}H_{57}NO_4Ti$: C, 70.23; H, 9.33; N, 2.27. Found: C, 69.75; H, 9.37; N, 2.27.

{TiMe[(O-2,4-Me$_2$C$_6$H$_2$-6-CH$_2$)$_2$(μ_2-OCH$_2$CH$_2$)N]}[Me$_2$Al(μ_2-O^{i}Pr)] (3a). AlMe$_3$ (0.5 mL, 1.0 mmol solution in Et$_2$O) was added dropwise at −30 °C to a toluene (10.0 mL) solution of **1a** (0.216 g, 1.0 mmol). The reaction mixture was stirred at room temperature for 3 h, and then the resultant volatiles were evaporated *in vacuo*, leaving an orange-yellow solid. The resultant solids were extracted with *n*-hexane (15 mL × 3). The orange solution was filtered, and the desired product was then collected as yellow microcrystals from the chilled solution (−30 °C). Yield: 0.245 g (97.0%). Nature: Yellow, crystalline solid. ^{1}H NMR ($CDCl_3$, 25 °C): δ −0.75 (s,

Table 7. Crystallographic Parameters for 3a and 3b[a]

	3a	3b
empirical formula	$C_{26}H_{40}AlNO_4Ti$	$C_{27}H_{42}AlNO_4Ti$
fw	505.49	519.51
cryst color, habit	yellow, block	yellow, block
cryst dimens	0.80 × 0.34 × 0.30 mm	0.30 × 0.14 × 0.06 mm
cryst syst	monoclinic	orthorhombic
lattice params	a = 8.4595(3) Å b = 21.2466(7) Å c = 15.3664(5) Å β = 100.0844(12)° V = 2719.22(16) Å^3	a = 16.1827(4) Å b = 15.6776(4) Å c = 22.2677(8) Å V = 5649.4(3) Å^3
space group	$P2_1/n$ (#14)	$Pbca$ (#61)
Z value	4	8
D_{calc}	1.235 g/cm^3	1.222 g/cm^3
F_{000}	1080.00	2224.00
μ(Mo Kα)	3.770 cm^{-1}	3.647 cm^{-1}
$2\theta_{max}$	54.9°	54.9°
no. of reflns measd	total: 26086; unique: 6154 (R_{int} = 0.024)	total: 50247; unique: 6410 (R_{int} = 0.067)
no. of observations ($I > 2.00(I)$)	4933	3107
no. of variables	338	349
residuals: R1 ($I > 2.00(I)$)	0.0394	0.0441
residuals: wR2 ($I > 2.00(I)$)	0.1219	0.1090
goodness of fit	1.009	1.009
max. peak in final diff map	0.36 e$^-$/Å^3	0.27 e$^-$/Å^3
min. peak in final diff map	−0.30 e$^-$/Å^3	−0.35 e$^-$/Å^3

[a] Diffractometer: Rigaku RAXIS-RAPID imaging plate. Structure solution: direct methods. Refinement: full-matrix least-squares. Function minimized: $\sum w(|F_o| - |F_c|)^2$ (w = least-squares weights). Standard deviation of an observation of unit weight: $[\sum w(|F_o| - |F_c|)^2/(N_o - N_v)]^{1/2}$ (N_o = number of observations, N_v = number of variables). Radiation: Mo Kα (λ = 0.71075 Å) graphite monochromated.

6H, $AlMe_2$), 1.27 (d, $J = 6$ Hz, 6H, $CH(CH_3)_2$), 1.35 (s, 3H, Ti−CH_3), 2.20 (s, 6H, Ar−CH_3), 2.32 (s, 6H, Ar−CH_3), 2.55 (t, 6 Hz, 2H, N−CH_2), 3.39−3.48 (m, 4H, CH_2−Ar), 3.71 (t, $J = 6$ Hz, 2H, CH_2−O), 4.78 (septet, $J = 6$ Hz, 1H, CH), 6.62 (s, 2H, Ar−H), 6.89 (s, 2H, Ar−H). ^{1}H NMR ($CDCl_3$, 55 °C): No change at elevated temperatures. ^{13}C NMR ($CDCl_3$, 25 °C): δ −8.38 (Al-(CH_3)$_2$), 16.28 (C(CH_3)$_2$, 20.60 (Ar−CH_3), 25.86 (Ar−CH_3), 58.89 (N−CH_2), 59.76 (Ti−CH_3), 61.28 (br, Ar−CH_2), 67.87 (O−CH_2), 71.46 (O−CH), 124.41, 124.81, 127.55, 129.10, 130.90, 158.72. Anal. Calcd for $C_{26}H_{40}AlNO_4Ti$: C, 61.78; H, 7.98; N, 2.77. Found: C, 62.31; H, 8.07; N, 2.67.

{TiMe[(O-2,4-Me$_2$C$_6$H$_2$-6-CH$_2$)$_2$(μ_2-OCH$_2$CH$_2$)N]}[Me$_2$Al(μ_2-O^{t}Bu)] (3b). Compound **3b** was prepared according to a procedure analogous to that given here for **3a** except $AlMe_3$ (1.0 mL, 1.0 mmol solution in ether) and **1b** (0.447 g, 1.0 mmol) were used. Nature: Yellow, crystalline solid. Yield: 0.466 g (89.4%). ^{1}H NMR ($CDCl_3$, 25 °C): δ −0.91 (m, 6H), 1.29 (s, 9H), 1.68 (m, 9H), 2.19 (s, 6H), 2.23 (s, 6H), 2.79 (m, 2H), 3.36−3.75 (m, 4H), 4.43−4.56 (m, 2H), 6.61−6.92 (m, 4H). ^{1}H NMR ($CDCl_3$, 55 °C): All the signals became very broad at higher temperature. ^{13}C NMR ($CDCl_3$, 25 °C): δ −8.00 (Al(CH_3)$_2$), 16.45 (Ar−CH_3), 20.58 (Ar−CH_3), 32.09 (C(CH_3)$_3$), 59.18 (N−CH_2), 61.27 (N−CH_2−Ar), 62.73 (Ti−CH_3), 67.78 (O−CH_2), 77.61 (O−C(CH_3)$_3$), 124.63, 127.45, 129.04, 130.91, 159.26. Anal. Calcd for $C_{30}H_{48}AlNO_4Ti$: C, 62.43; H, 8.15; N, 2.70. Found: C, 62.59; H, 8.36; N, 2.68.

Crystallographic Analysis. All measurements were made on a Rigaku RAXIS-RAPID imaging plate diffractometer with graphite-monochromated Mo Kα radiation. All structures were solved by direct methods and expanded using Fourier techniques,[29] and the non-hydrogen atoms were refined anisotropically. Hydrogen atoms were included but not refined. All calculations for complexes **1a**, **1b**, **2a**, **2b**, **3a**, and **3b** were performed using the Crystal Structure[30] crystallographic software package. Selected crystal collection parameters are summarized in Tables 6 and 7.

Polymerization of Ethylene. Ethylene polymerizations were conducted in toluene or in *n*-octane by using a 100 mL scale autoclave. Solvent (29.0 mL) and d-MAO (3.0 mmol) prepared by removing toluene and $AlMe_3$ from the commercially available MAO (PMAO-S, Tosoh Finechem Co.) were charged into the autoclave in the drybox, and the apparatus was placed under an ethylene atmosphere (1 atm). After the addition of toluene or *n*-octane solution (1.0 mL) containing **1a** via a syringe, the reaction apparatus was pressurized to 8 atm, and the mixture was stirred magnetically for 10 or 60 min. After the above procedure, ethylene was purged, and the mixture was then poured into EtOH (150 mL) containing HCl (10 mL). The resultant polymer was collected on a filter paper by filtration and was adequately washed with EtOH and then dried *in vacuo*. Polymerization results in Table 4 are at the optimized Al/Ti molar ratios.

Acknowledgment. S.P. and K.N. dedicate this paper to the late Prof. G. Sundararajan (Indian Institute of Technology Madras, deceased in February 2007) in honor of his remarkable contributions to this research field. K.N. would like to express his heartfelt thanks to Tosoh Finechem Co. for donating MAO-(PMAO-S), and to Prof. Michiya Fujiki (NAIST) for helpful comments. The present research is partly supported by a Grant-in-Aid for Scientific Research (B) from the Japan Society for the Promotion of Science (JSPS, No. 18350055).

Supporting Information Available: Crystal structure determinations, reports for **1a**,**b**, **2a**,**b**, and **3a**,**b**; the crystallographic data are also given as CIF files. These materials are available free of charge via the Internet at http://pubs.acs.org.

OM0611507

(29) DIRDIF94: Beurskens, P. T.; Admiraal, G.; Beurskens, G.; Bosman, W. P.; de Delder, R.; Israel, R.; Smits, J. M. M. *The DIRDIF94 program system*; Technical report of the crystallography laboratory; University of Nijmegen: The Netherlands, 1994.

(30) (a) *Crystal Structure 3.6.0*, Crystal Structure Analysis Package; Rigaku and Rigaku/MSC: The Woodlands, TX, 2000−2004. (b) Watkin, D. J.; Prout, C. K.; Carruthers, J. R.; Betteridge, P. W. *CRYSTALS Issue 10*; Chemical Crystallography Laboratory: Oxford, UK, 1996.